

ChemComm

Accepted Manuscript



This is an *Accepted Manuscript*, which has been through the Royal Society of Chemistry peer review process and has been accepted for publication.

Accepted Manuscripts are published online shortly after acceptance, before technical editing, formatting and proof reading. Using this free service, authors can make their results available to the community, in citable form, before we publish the edited article. We will replace this *Accepted Manuscript* with the edited and formatted *Advance Article* as soon as it is available.

You can find more information about *Accepted Manuscripts* in the [Information for Authors](#).

Please note that technical editing may introduce minor changes to the text and/or graphics, which may alter content. The journal's standard [Terms & Conditions](#) and the [Ethical guidelines](#) still apply. In no event shall the Royal Society of Chemistry be held responsible for any errors or omissions in this *Accepted Manuscript* or any consequences arising from the use of any information it contains.

Cite this: DOI: 10.1039/c0xx00000x

www.rsc.org/xxxxxx

ARTICLE TYPE

Non-aggregated and tumour-associated macrophage-targeted photosensitiser for photodynamic therapy: A novel zinc(II) phthalocyanine containing octa-sulphonates

Xing-Shu Li, Mei-Rong Ke, Miao-Fen Zhang, Qing-Qing Tang, Bi-Yuan Zheng and Jian-Dong Huang*

Received (in XXX, XXX) Xth XXXXXXXXX 20XX, Accepted Xth XXXXXXXXX 20XX

DOI: 10.1039/b000000x

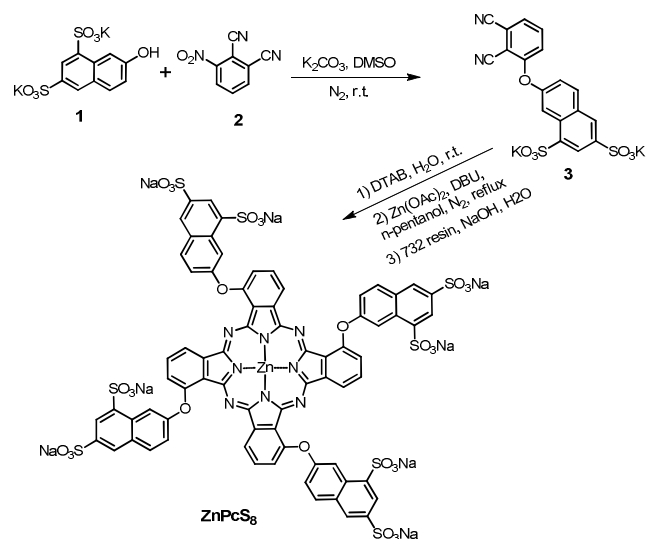
A novel zinc(II) phthalocyanine bearing octa-sulphonates has been prepared, which is non-aggregated in water, highly photoactive and low dark-toxic. More interestingly, it exhibits specific affinity to macrophage via the scavenger receptor-A, and can selectively accumulate in tumour site.

Macrophages are highly abundant in the stroma of a series of solid tumours including breast, ovarian, pancreatic and hepatocellular carcinomas.^{1,2} The macrophages in tumour tissue (named as tumour-associated macrophages, TAMs) have been shown to play a crucial role in the development and progression of cancer. In particular, they produce a plethora of cytokines to induce cancer cell migration, facilitate angiogenesis and reconcile immunosuppression.³⁻⁵ Therefore, TAMs have emerged as a promising target for cancer treatment.^{6,7}

Among kinds of therapeutic approaches focused on TAMs, macrophage-targeted photodynamic therapy exhibits especially fascinating prospect due to its special dual selectivity.⁸⁻¹⁰ Photodynamic therapy (PDT) destroys target cells through the combined action of a photosensitiser and molecular oxygen upon irradiation with light to generate reactive oxygen species (ROS), particularly singlet oxygen.^{11,12} By means of macrophage-targeting of a photosensitiser and selectively illuminating the tumour tissue, TAM-targeted PDT would result in a desirable therapeutic effect including enhancement of the potency of PDT as well as circumvention of the damage to the macrophages in normal tissues. The overall efficacy of this treatment depends greatly on the behaviour of photosensitisers, including its selectivity towards macrophages and efficiency to generate ROS. However, only a few functionalized photosensitisers have been reported so far which show specific affinity to TAMs.^{8,9,13-15} In particular, TAM-targeted photosensitisers without conjugation with biomacromolecules have scarcely been revealed.¹⁴ On the other hand, most of the photosensitisers with strong absorption in near infrared region are conjugated compounds, such as porphyrin, porphyrin and phthalocyanine derivatives. They often showed strong aggregation in aqueous media and slow *in vivo* clearance (in particular, highly retained in the livers), which hence resulted in greatly reducing of the photosensitising efficiency and potential side-effects such as hepatic necroses.¹⁶⁻¹⁸ Thus, developing non-aggregated, rapidly eliminated and TAM-targeted

photosensitisers for PDT is a very challenging and meaningful work.

We herein display the synthesis and characterisation of a novel zinc(II) phthalocyanine tetra-substituted with 6,8-disulphonate-2-naphthoxy (ZnPcS₈) (see in Fig. 1). Introduction of eight highly water-soluble and negative-charged sulphonates facilitates this phthalocyanine having favourable properties for PDT, including (1) non-aggregation and high singlet oxygen quantum yield in water; (2) low dark toxicity and high therapeutic index; (3) more importantly, specific affinity to the macrophage via the scavenger receptor-A (SR-A), and enhanced selectivity to tumour tissue; (4) fast excretion from body after PDT effect to minimise potential side-effects.



Scheme 1. Synthetic route of ZnPcS₈. (To simplify the scheme, here only the major C_{4h} isomers were showed for tetra-substituted phthalocyanines, which likely present the other isomers)

The octa-sulphonate ZnPcS₈ was prepared as shown in Scheme 1. The precursor of disulphonate-substituted phthalonitrile **3** was first prepared by a nucleophilic substitution reaction between potassium 2-naphthol-6,8-disulphonate (**1**) and 3-nitrophthalonitrile (**2**) in the presence of K₂CO₃ in dry DMSO. The precursor **3** was then treated with dodecyl trimethyl ammonium bromide (DTAB), followed by encountering a zinc

ion-mediated cyclotetramerisation using 1,8-diazabicyclo-[5.4.0]undec-7-ene (DBU) as a catalyst in *n*-pentanol to afford the final product ZnPcS₈, which was purified by silica gel column chromatography, cation-exchange resin and size-exclusion chromatography. It is worth to mention that ZnPcS₈ could not be successfully obtained according to the general cyclisation procedure described previously,¹⁹ maybe due to the low solubility of **3** in *n*-pentanol and electrostatic repulsion interaction between the peripheral sulphonate anions. Thus, cationic surfactant DTAB was used in the reaction to form ion pairs with the sulphonate anions, and then circumvent these problems. The new compound ZnPcS₈ was well characterised with IR, ¹H NMR, HRMS and elemental analysis (see in ESI†).

The spectroscopic properties of ZnPcS₈ were measured in *N,N*-dimethyl formamide (DMF). As shown in Fig. 1a, the UV-vis spectrum of ZnPcS₈ is typical for non-aggregated phthalocyanines with an intense and sharp Q-band at 696 nm. Upon excitation at 610 nm, ZnPcS₈ shows a strong fluorescence emission at 705 nm with a fluorescence quantum yield (Φ_f) of 0.14 relative to unsubstituted zinc(II) phthalocyanine (ZnPc, $\Phi_f = 0.28$ ²⁰) (see Fig. 1b and Table 1). On the other hand, the octaanionic ZnPcS₈ is readily soluble in water, giving similar spectroscopic properties with that in DMF (Fig. 1 and Table 1). As shown in Fig S1 (ESI†), the Q-band of ZnPcS₈ in water well obeys the Lambert-Beer law, indicating that ZnPcS₈ essentially remains a monomer form in aqueous solution without any surfactant as a result of its extremely high hydrophilicity and electrostatic repulsion interaction of the highly negative charged substituents. Due to the strong hydrophobic interactions of macrocycle π systems, phthalocyanines generally tend to aggregate in aqueous media, leading to great reduction of photosensitising efficiency.^{21,22} Even for tetra-sulphonate phthalocyanines, the aggregated trends were also observed in water without surfactant or organic solvent.^{23,24} In fact, zinc(II) phthalocyanine remained a monomer form in aqueous solution in absence of disaggregating agents is rarely reported.^{14,25-27} Thus, the favourable non-aggregated property of ZnPcS₈ in aqueous solutions makes it a good candidate as an ideal photosensitiser for PDT.

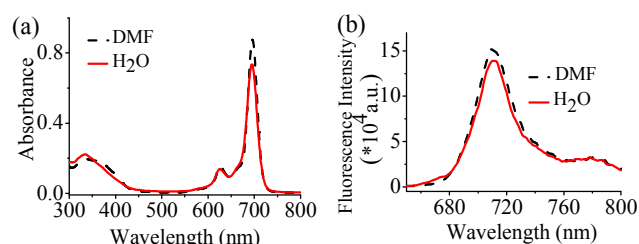


Fig. 1 (a) UV-vis and (b) fluorescence spectra of ZnPcS₈ (4 μ M) in DMF or water.

Table 1 Photophysical and photochemical data for ZnPcS₈

Solvent	λ_{max} (nm)	λ_{em} (nm) ^a	$\epsilon \times 10^5$ (M ⁻¹ cm ⁻¹)	Φ_f ^b	Φ_Δ
DMF	696	705	2.17	0.14	0.82 ^c
Water	695	708	1.84	0.12	0.62 ^d

^a Excited at 610 nm. ^b Using ZnPc in DMF as the reference ($\Phi_f = 0.28$). ^c Determined using DPBF as chemical quencher, and ZnPc in DMF as the reference ($\Phi_\Delta = 0.56$). ^d Determined using DPBF as chemical quencher, and MB in D₂O as the reference ($\Phi_\Delta = 0.52$).

As shown in Table 1, the singlet oxygen quantum yield (Φ_Δ) of ZnPcS₈ was determined as 0.82 in DMF relative to ZnPc ($\Phi_\Delta = 0.56$) by a steady-state method using 1,3-diphenylisobenzofuran (DPBF) as the scavenger.²⁸ This shows that ZnPcS₈ is a high efficient singlet oxygen generator in DMF. Moreover, the Φ_Δ of ZnPcS₈ was also evaluated in aqueous solution as shown in Fig. S2 (ESI†). In contrast to methylene blue (MB) ($\Phi_\Delta = 0.52$ ²⁹), ZnPcS₈ still shows a high Φ_Δ of 0.62 in D₂O, which can be attributed to its non-aggregated property in aqueous solution.

The macrophage-targeting effects of ZnPcS₈ were first investigated by *in vitro* cell studies. The dark toxicity and photodynamic activities of ZnPcS₈ were examined against two different cell lines, namely mouse macrophages J774A.1 and human hepatocellular carcinoma HepG2 cells by a colorimetric 3-(4,5-dimethyl-2-thiazolyl)-2,5-diphenyl-2H-tetrazolium bromide (MTT) assay.³⁰ The J774A.1 cell line, which is able to highly express SR-A was used as a model for the study of SR-mediated endocytosis,^{31,32} while HepG2 cells, without expression of SR-A, are chosen as a negative control. It can be seen from Fig. S3 (ESI†) that ZnPcS₈ is essentially non-cytotoxic even at 600 μ M towards both cell lines in the absence of light, with TC₅₀ values, defined as the dye concentrations required to kill 50% of the cells in the dark, ranging from 1500 μ M to more than 2000 μ M (Table 2). On the other hand, upon illumination with red light, ZnPcS₈ could induce a highly efficient photodynamic effect on J774A.1 cells with an EC₅₀ value, defined as the dye concentrations required to kill 50% of the cells with light, of 0.28 μ M. It is noteworthy that the ratio of TC₅₀/EC₅₀ (“therapeutic index”) reached over 5000 for J774A.1 cells, which is an excellent prerequisite for a successful drug. However, the compound shows remarkably decreased photocytotoxicity against the SR-A-negative HepG2 cells, having a more than 13-fold higher EC₅₀ value in contrast to that against J774A.1 cells (see Fig. 2 and Table 2).

Table 2 EC₅₀ and TC₅₀ values for ZnPcS₈ against HepG2 and J774A.1 cells

Cell	EC ₅₀ (μ M)	TC ₅₀ (μ M)
HepG2	3.78	>2000
J774 A.1	0.28	1500

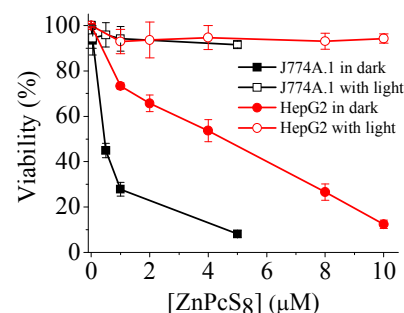


Fig. 2 Cytotoxic effects of ZnPcS₈ on J774A.1 and HepG2 cells in the absence (open symbol) and presence (closed symbol) of light ($\lambda > 610$ nm) at a dose of 27 J·cm⁻². Data are expressed as mean \pm standard deviation (SD) ($n = 3$).

To explain the different photocytotoxicity, the cellular uptake of ZnPcS₈ by HepG2 and J774A.1 cells was compared by

confocal laser scanning microscopy (CLSM) analysis as shown in Fig. 3. It is clear that the intracellular fluorescence intensity of ZnPcS₈ in J774A.1 cells is significantly stronger, which is about 7-fold higher compared to that in HepG2 cells, suggesting a higher cellular uptake for J774A.1 cells. Hence, the higher photocytotoxicity of ZnPcS₈ against J774A.1 cells can be attributed to its higher cellular uptake.

It is known that SR-A could bind a wide range of polyanionic ligands, including polyribonucleotides, polysaccharides and glycosylated proteins.^{33,34} To confirm the cellular uptake of octa-anionic ZnPcS₈ by J774A.1 cells is through a SR-A-mediated process, a competitive assay of cellular uptake of J774A.1 cells was performed in the presence of polyinosinic acid (poly I), a specific ligand to SR-A.³⁴ As shown in Fig. 4a and Fig. S4 (ESI[†]), the intracellular fluorescence intensity gradually decreased with the increase of poly I. After co-incubation with 100 μg·mL⁻¹ of poly I, the fluorescence intensity was weakened to *ca.* 30% relative to that without poly I, suggesting that the cellular uptake of ZnPcS₈ by J774A.1 cells was significantly inhibited by poly I. On the other hand, the inhibitory effect of poly I on photocytotoxicity was further confirmed by a MTT assay. It can be seen from Fig. 4b that the inhibitory effect also presents a dose-dependent result. The EC₅₀ values change from 0.28 μM to 2.22 μM after co-incubation with 100 μg·mL⁻¹ of poly I. However, as shown in Fig. S5 (ESI[†]), for SR-A-negative HepG2 cells, both the intracellular fluorescence intensity and photocytotoxicity of ZnPcS₈ are comparable with that in the presence of poly I, suggesting that both the cellular uptake and photodynamic activity of ZnPcS₈ are not impeded by poly I. Thus, we can conclude that the SR-A is mainly responsible for the cellular uptake and subsequent photoinactivity towards J774A.1 cells.

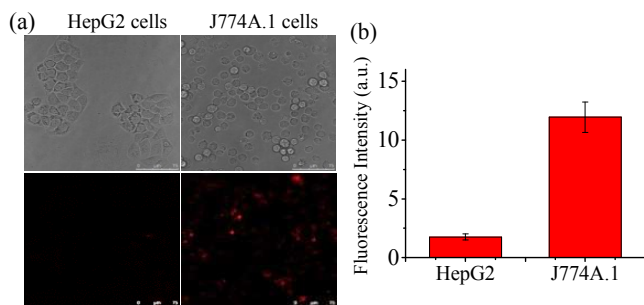


Fig. 3 (a) Bright field (up row) and intracellular fluorescence (down row) images of HepG2 and J774A.1 cells after incubation with ZnPcS₈ (1 μM) for 2 h. (b) Comparison of the corresponding average intracellular fluorescence intensities. Data are expressed as the mean ± SD (number of cells = 50).

To test the effect of the number of negative charges of a photosensitizer on the SR-A-mediated cellular uptake, a competitive assay was also performed on another zinc(II) phthalocyanine analogue containing only four sulphonates (ZnPcS₄, see Fig. S6, ESI[†]).³⁵ As shown in Fig. S7 (ESI[†]), the intracellular fluorescence intensities hardly change in the presence of poly I for both HepG2 and J774A.1 cells, meaning that the cellular uptakes of ZnPcS₄ are not impeded by the poly I. The results suggest that, even for the SA-R-positive J774A.1 cells, the cellular uptake of the tetra-anionic ZnPcS₄ should not be through a SR-A-mediated process. Therefore, in view of the

different uptake processes of ZnPcS₈ and ZnPcS₄, we preliminarily conclude that it should need much more negative charges for phthalocyanine-based photosensitizers to trigger the SR-A-mediated endocytosis.

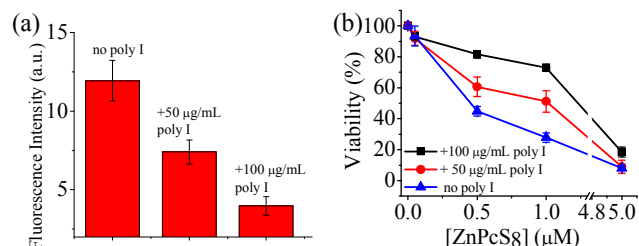


Fig. 4 (a) Comparison of the average intracellular fluorescence intensities of ZnPcS₈ (1 μM) in J774A.1 cells in the absence and presence of poly I. Data are expressed as the mean ± SD (number of cells = 50). (b) The photocytotoxicities of ZnPcS₈ against J774A.1 cells in the absence (■) and presence of 50 μg·mL⁻¹ (●) or 100 μg·mL⁻¹ (▲) poly I. Data are expressed as mean ± SD (*n* = 3).

The subcellular localisation of ZnPcS₈ was also investigated on both cell lines by using fluorescence microscopy. The cells were first incubated with ZnPcS₈, followed by being stained with Mito-Tracker Green and Lyso-Tracker Red. As shown in Fig. S8 (ESI[†]), the fluorescence of ZnPcS₈ in HepG2 cells was well overlapped with the fluorescence of Lyso-Tracker but not with that of Mito-Tracker, showing that ZnPcS₈ is mainly localised in lysosomes. For J774A.1 cells, obviously superimposed fluorescence signals were observed for ZnPcS₈ and the two probes, indicating that ZnPcS₈ could accumulate in both lysosomes and mitochondria.

Finally, the biodistribution of ZnPcS₈ was demonstrated *in vivo*. Nude mice bearing a HepG2 tumour were treated with an intravenous dose of ZnPcS₈ (~1 nmol·g⁻¹). Their fluorescence images were monitored continuously up to 24 h (as shown in Fig. 5a). Shortly after injection, ZnPcS₈ spread throughout the whole body. After 10 min post-injection, most of the fluorescence signals in the body started to decline gradually in intensity, while the fluorescence intensity in tumour site kept strengthening and reached the maximum fluorescence at 4 h. After 24 h, nearly no fluorescence signal was observed in the whole body except for the tumour site, suggesting that ZnPcS₈ could be not only selectively localised in tumour site, but also metabolised and cleared from the body quickly. To further confirm the distribution of ZnPcS₈ in different organs, the nude mice were sacrificed after 24 h, and then the fluorescences of tumour and other organs, including heart, liver, kidney, lung and spleen were compared, as shown in Fig. 5b. It was clear that the fluorescence of ZnPcS₈ can be seen only in tumour, liver and kidney. The quantitative analysis revealed that the average fluorescence intensity in the tumour region is about 6-fold and 3-fold higher than that in liver and kidney, respectively. It's obvious that ZnPcS₈ has a highly specific affinity to tumour over normal tissues.

As aforementioned, TAMs are an abundant part of solid and haematological malignancies. Moreover, TAMs were found to be high expression of SR-A^{36,37}. Thus, considering the affinity to J774A.1 cells via the SR-A, we speculate that the high tumour

specificity of ZnPcS₈ may be through the TAM-mediated mechanism, but it needs to be further investigated.

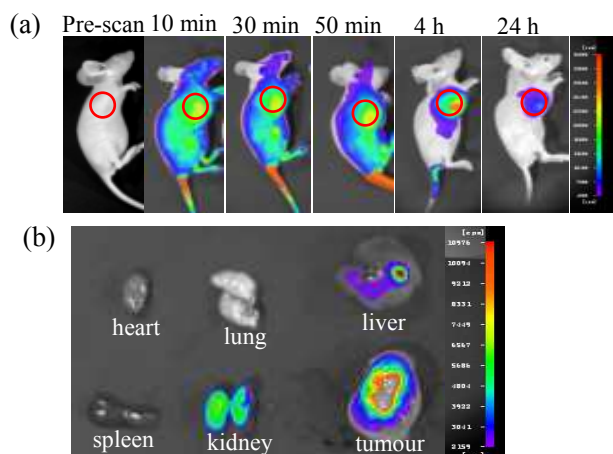


Fig. 5 (a) Fluorescence images of tumour-bearing nude mice before and after intravenous injection of ZnPcS₈. The red circles indicate tumor sites. (b) *In vivo* distribution of ZnPcS₈ in tumour and different organs of the nude mice after 24 h post-injection.

In summary, we have synthesised and characterised a novel octa-sulphonate-functionalised zinc(II) phthalocyanine (ZnPcS₈) and evaluated its *in vitro* photodynamic activities against J774A.1 and HepG2 cells. Apart from the excellent photophysical and non-aggregated features in water, ZnPcS₈ with strongly negative charges is favorable for the specific affinity to macrophage cell via the SR-A. The *in vivo* studies confirm the specificity of ZnPcS₈ to tumour tissues. In addition, the highly hydrophilic photosensitizer facilitates its rapid elimination from the body of nude mice. The overall results show that the macrophage-targeted ZnPcS₈ is a highly promising photosensitizer, which may provide a novel strategy for targeted PDT.

This work was supported by the Natural Science Foundation of China (Grant Nos. 21172037, 21301031 and 21473033), and Specialized Research Fund for the Doctoral Program of Higher Education (Grant No. 20113514110001).

Notes and references

College of Chemistry, State Key Laboratory of Photocatalysis on Energy and Environment, Fuzhou University, Fuzhou 350108, China.

* Corresponding author, e-mail address: jdhuang@fzu.edu.cn

Electronic Supplementary Information (ESI) available: synthesis, characterisation and experimental details. See DOI: 10.1039/b000000x/

1. Y. Wu and L. Zheng, *Cancer Microenviron.*, 2012, **5**, 195-201.
2. C. Feig, A. Gopinathan, A. Neeße, D. S. Chan, N. Cook and D. A. Tuveson, *Clin. Cancer Res.*, 2012, **18**, 4266-4276.
3. R. A. Franklin, W. Liao, A. Sarkar, M. V. Kim, M. R. Bivona, K. Liu, E. G. Pamer and M. O. Li, *Science*, 2014, **344**, 921-925.
4. D. Hanahan and R. A. Weinberg, *Cell*, 2011, **144**, 646-674.
5. D. F. Quail and J. A. Joyce, *Nat. Med.*, 2013, **19**, 1423-1437.
6. T. L. Rogers and I. Holen, *J. Transl. Med.*, 2011, **9**, 177-193.
7. A. Sica, T. Schioppa, A. Mantovani and P. Allavena, *Eur. J. Cancer*, 2006, **42**, 717-727.
8. T. N. Demidova and M. R. Hamblin, *Int. J. Immunopathol. Pharmacol.*, 2004, **17**, 117-126.
9. M. R. Hamblin, J. L. Miller and B. Ortel, *Photochem. Photobiol.*,

- 2000, **72**, 533-540.
10. N. Rousset, L. Bourre and S. Thibaud, *Sensitizers in Photodynamic Therapy*, ed. T. Patrice, The Royal Society of Chemistry, London, 2003, vol. 2, p. 59.
11. A. P. Castano, P. Mroz and M. R. Hamblin, *Nat. Rev. Cancer*, 2006, **6**, 535-545.
12. Á. Juarranz, P. Jaén, F. S. Rodríguez, J. Cuevas and S. González, *Clin. Transl. Oncol.*, 2008, **10**, 148-154.
13. N. Bresseur, R. Langlois, G. L. Madeleine, R. Ouellet and J. E. van Lier, *Photochem. Photobiol.*, 1999, **69**, 345-352.
14. C. F. Choi, P. T. Tsang, J. D. Huang, E. Y. Chan, W. H. Ko, W. P. Fong and D. K. P. Ng, *Chem. Commun.*, 2004, 2236-2237.
15. W. M. Sharman, J. E. van Lier and C. M. Allen, *Adv. Drug Deliver. Rev.*, 2004, **56**, 53-76.
16. N. Kobayashi and W. A. Nevin, *Appl. Organomet. Chem.*, 1996, **10**, 579-590.
17. M. R. Detty, S. L. Gibson and S. J. Wagner, *J. Med. Chem.*, 2004, **47**, 3897-3915.
18. W. Liu, N. Chen, H. Jin, J. Huang, J. Wei, J. Bao, C. Li, Y. Liu, X. Li and A. Wang, *Regul. Toxicol. Pharmacol.*, 2007, **47**, 221-231.
19. M. R. Ke, J. D. Huang and S. M. Weng, *J. Photoch. Photobio. A*, 2009, **201**, 23-31.
20. I. Scalise and E. N. Durantini, *Bioorg. Med. Chem.*, 2005, **13**, 3037-3045.
21. J. R. Darwent, P. Douglas, A. Harriman, G. Porter and M. C. Richoux, *Coord. Chem. Rev.*, 1982, **44**, 83-126.
22. A. W. Snow. Phthalocyanine Aggregation. In *The Porphyrin Handbook*; Kadish, K. M., Smith, K. M., Guillard, R., Eds.; Academic Press: San Diego, 2003, Vol. 17, p. 129.
23. L. Howe and J. Z. Zhang, *Photochem. Photobiol.*, 1998, **67**, 90-96.
24. V. Iliev, V. Alexiev and L. Bilyarska, *J. Mol. Catal. A: Chem.*, 1999, **137**, 15-22.
25. S. Makhseed, M. Machacek, W. Alfadly, A. Tuhl, M. Vinodh, T. Simunek, V. Novakova, P. Kubat, E. Rudolf and P. Zimcik, *Chem. Comm.*, 2013, **49**, 11149-11151.
26. M. K. Gümüstas, B. S. Sesalan, P. Atukeren, B. Yavuz and A. Gül, *J. Coord. Chem.*, 2010, **63**, 4319-4331.
27. W. Liu, T. J. Jensen, F. R. Fronczek, R. P. Hammer, K. M. Smith and M. G. H. Vicente, *J. Med. Chem.*, 2005, **48**, 1033-1041.
28. M. D. Maree, N. Kuznetsova and T. Nyokong, *J. Photoch. Photobio. A*, 2001, **140**, 117-125.
29. R. W. Redmond and J. N. Gamlin, *Photochem. Photobiol.*, 1999, **70**, 391-475.
30. H. Tada, O. Shiho, K. Kuroshima, M. Koyama and K. Tsukamoto, *J. Immunol. Methods*, 1986, **93**, 157-165.
31. Y. Chao, P. P. Karmali, R. Mukthavaram, S. Kesari, V. L. Kuznetsova, I. F. Tsigelny and D. Simberg, *ACS Nano*, 2013, **7**, 4289-4298.
32. P. Piccolo, P. Annunziata, P. Mithbaokar and N. B. Pierri, *Gene Ther.*, 2014.
33. C. Neyer, A. Pluddemann, S. Mukhopadhyay, E. Maniati, M. Bossard, S. Gordon and T. Hagemann, *J. Immunol.*, 2013, **190**, 3798-3805.
34. H. E. de Vries, A. C. E. Moor, T. M. A. R. Dubbelman, T. J. C. van Berkel and J. Kuiper, *J. Pharmacol. Exp. Ther.*, 1999, **289**, 528-534.
35. X.-S. Li, M.-R. Ke, W. Huang, C.-H. Ye, and J.-D. Huang, *Chem. Eur. J.*, 2015, DOI: 10.1002/chem.201404514.
36. A. Mantovani, S. Sozzani, M. Locati, P. Allavena and A. Sica, *Trends Immunol.*, 2002, **23**, 549-555.
37. T. Hagemann, J. Wilson, F. Burke, H. Kulbe, N. F. Li, A. Pluddemann, K. Charles, S. Gordon and F. R. Balkwill, *J. Immunol.*, 2006, **176**, 5023-5032.